IJE TRANSACTIONS B: Applications Vol. 33, No. 11, (November 2020) 2384-2398

International Journal of Engineering

Journal Homepage: www.ije.ir

Regression Modeling and Process Analysis of Plug and Spot Welds Used in Automotive Body Panel Assembly

T. Saeheaw*

Department of Teacher Training in Mechanical Engineering, Faculty of Technical Education, King Mongkut's University of Technology North Bangkok, Bangkok, Thailand

P A P E R I N F O

Paper history:
Received 30 May 2020
Received in revised form 06 August 2020
Accepted 03 September 2020

Keywords:
Automotive Body Panel
Genetic Algorithm
Plug Weld
Spot Weld
Tensile Strength

A B S T R A C T

Resistance spot welding is the primary welding process used in automotive body panel assembly. However, plug welding is widely used in automotive body repair due to its technical simplicity and cost benefits. In this paper, spot welding and plug welding using Tungsten Inert Gas (TIG) welding of an automotive body panel are compared. TIG welding is selected for plug welding because it offers the greatest flexibility to weld the widest range of materials, thicknesses, and types. The base material used in this study is JIS G3141 SPCC. Full factorial experimental design coupled with statistical and graphical analysis of the results using analysis of variance was applied to determine the significance of process parameters. Parameter interactions were investigated using regression analysis, model adequacy checks, and determination of optimum conditions. A genetic algorithm is used to predict the optimum combination of the process parameters to realize the highest strength level. For tensile-shear strength, the experimental results demonstrate that plug welding has a higher maximum load than spot welding. The optimum plug welding joints were obtained at a hole diameter of 9 mm and a welding current of 136 kA, with a maximum load of 8.2 kN. The maximum load of the spot weld joint, 7.4 kN, was found at a welding current of 70 kA, an electrode force of 0.25 MPa, and 10 cycles of welding time.

***doi**: 10.5829/ije.2020.33.11b.29*

1. INTRODUCTION

Joining is a pivotal characteristic in automobile design. Generally, joints represent the weakest areas in an automobile's structure and often represent the initiation location for failures in service. Strength of the joints often determines the reliability and quality of a manufactured product. The development and application of new materials, compounded with welding optimization and structural optimization design, has allowed automobile body manufacturing technology to secure sufficient rigidity and safety performance. Nonetheless, in cases in where damage is caused by collisions, body damage restoration technology sees itself exceeded by the manufacturer's body manufacturing technology. The efficiency of body damage restoration technology is highly dependent on an expert's skill and cannot be accessed quantitatively and objectively [1].

We can distinguish between the following processes in body repair work: (1) damage analysis and diagnosis, (2) measurement and correction of the vehicle system, (3) panel replacement and correction, (4) painting and rust prevention, and (5) technical analysis. Appropriate equipment is used in all processes. Body repair work highly relies on the method and type of welding. In order to guarantee the safety of a vehicle in operation, an optimized repair technique should take into consideration both welding and structural characteristics [2].

Spot welding is viable for short-time welds. Spot welding allows a smal area to be heated, making heat deformation a negligible part of the process. Moreover, reproducibility of the weld's quality is excellent. Nonetheless, the welded material and its thickness must be taken into consideration. In order to join metals together , it is important to apply pressure at both sides

*Corresponding Author Institutional Email: *teerapun.s@fte.kmutnb.ac.th* (T. Saeheaw)

Please cite this article as: T. Saeheaw, Regression Modeling and Process Analysis of Plug and Spot Welds Used in Automotive Body Panel Assembly, International Journal of Engineering (IJE), IJE TRANSACTIONS B: Applications Vol. 33, No. 11, (November 2020) 2384-2398

of the joint, thus causing localized heating at the interface [3]. The safety design and durability of a vehicle are significantly affected by the failure performance and characteristics of spot welds. Even though spot welding is not extensively used, plug welding is commonly used as well. Plug welding uses a weld metal to fill a hole in the middle of a panel. The first step is to make a round hole in the outer sheet. Next, the hole is filled with a weld metal and panels are joined using arc spot welding, also called argon gas (Ar) welding. With plug welding, joining through one side of the panel becomes possible, thus making the usable range wider than the one achieved through spot welding [4]. Nonetheless, both spot and plug welding can be done regardless of the workpiece's position. While the load caused by a motor vehicle accident damages the vehicle body panel, weld seam damages are often generated by the action of shear loading.

2. LITERATURE REVIEW

RSW (Resistance spot welding) is the dominant process used to join thin sheet steel metal components by fusing discrete spots at the interface of a workpiece utilized for low-carbon steel body construction in crash repair and automotive production. A reliable, cost-effective, rapid, and automated process, RSW does not require noticeable operator skills. Nonetheless, RSW has a major flaw, i.e., inconsistency of quality from weld to weld. The complexity generated by numerous sources of variability increases production costs, complicates automation, and reduces weld quality [5]. Consequently, the parameters that affect weld quality must be determined and controlled.

When using RSW, electric current passes through two electrodes. Sheets are locally joined by their liquid phases produced due to Joule heating (I^2R), a process that generates melting and the production of a nugget. During the welding operation, the sheets are held together by the pressure from the electrode tips, creating fusion bonding at the atomic level between the materials. The joint forms when the fusion-bonded liquid phase cools under pressure. A typical fusion weld consists of the heat-affected zone and the fusion zone. RSW involves various parameters that can influence the mechanical performance and weldability of weldments. The weld nugget and the nugget's strength are controlled by weld parameters that significantly affect the weld quality. These parameters include electrode force, weld current, and welding time [6]. The Precision Metalforming Association provides not only valuable information about these dimensions but also straightforward guidance on the material types for spot welds. The nugget is also influenced by the electron tip design and the surface conditions set between the sheets. The diameter of the weld nugget is usually less than the diameter of the impressions electrodes create on the material. Nonetheless, standards vary in regard to the range of parameters that are usually applied for specific materials. When a new RSW process is set up, it is necessary to set optimum parameters using a standard as a guideline. It is also necessary to verify the weld quality by destructive testing. The strength of a single spot-welded lap joint depends on properties of the base material and welding parameters. These factors influence the welds' mechanical behavior [7-9].

If certain conditions are met, using plug welds can be more advantageous than other types of welds [10]. The use of plug-welded joints is very popular in steel structures. An alternative to spot welding, plug welding is used by vehicle manufacturers if there is not sufficient access for a spot welder (i.e. double-sheeting structures, constructions with a profile stiffener, and complex structures). When plug welding is used, the connection is produced by the weld in the contact surface of adjoining parts and on the walls of circular openings. If done properly, plug welds can be stronger than the initial spot welds. In DIY (do it yourself) car restoration, plug welding is used instead of spot welding. It is usually done on panel flanges that have been initially spot-welded. This weld type is notably suitable in difficult maintenance conditions of welded constructions. Usually, plug welds are applied at the centre of doubler plates for lap joints. One of the doubler plates has round holes. Typically, welds start around the perimeter of the hole and spiral to the centre, using either another member behind the hole or backing. This type of welds avoids the buckling of lapped parts and transfers load by shear. In this type of welding, uniform fusion to the roots of the joints is required. To form the joint, weld metal is placed in the holes, penetrating and fusing with the base metal of the members. In order for the adjacent weld to easily melt the slag, the weld must be done quickly. Nonetheless, slag inclusions are commonplace. Weld shrinkage during cooling and solidification is one of the biggest problems with plug welds. This shrinkage produces significant residual stresses at the centre of the plug, which solidifies last. This causes micro-cracks in the original weld, alongside near–yield point residual stresses that could trigger cracking as a consequence of the applied stresses on the structure. The applied stresses are considerably less than the anticipated fatigue limit.

Rolls-Royce Motors[2] highly recommends the use of RSW, TIG welding, and metal inert gas (MIG) in the replacement of underframe and body panels. In MIG welding, a reel of filler wire is fed continuously by means of a welding torch under a shield of inert gas.

[2] http://heritage.bentleymotors.com/en/technical-library/download/TSD4600.pdf. Accessed 19 October 2019

The weld is protected from the atmosphere by the gas that surrounds the weld pool and the arc. When used for body repair work, MIG welding provides an important advantage: it generates a limited heated weld area. As a consequence, the distortion and contraction stresses are minimal. MIG welding equipment is suitable for intermittent, continuous, and plug welds. In order to achieve an adequate weld, it is necessary to clean to bare metal the areas of the panels that need to be welded. Additionally, any trace of sealing materials, grease, or paint needs to be removed. In the case of TIG welding, a tungsten electrode is attached to the welding torch. The torch supplies the inert gas to the weld area, while the filler wire is fed manually. The weld is protected from the atmosphere by the gas that surrounds the weld pool and the arc. Among all the welding processes, TIG welding is the most flexible. It produces the best-penetrating and cleanest welds, can be used on any type of material, and enables more control over the way the weld lays down. In the case of stick welding or MIG welding, the filler material functions as the electrode, i.e., it continuously feeds filler material inside the puddle. As opposed to other welding processes, the use of TIG welding allows welders to slow down, use filler, and work the puddle until they achieve the size and the look of weld they need. Apart from controlling the amount of added filler, welders can also control how much heat is put into the workpiece. This could turn into a significant advantage in those situations in which welders need to bridge a large gap and must add a considerable amount of filler material. In this context, the weld moves along gradually and begins to overheat. This allows welders to back off the pedal while still maintaining the arc and gas coverage, cool down the puddle, and continue welding. As a result, TIG welding is particularly suitable for filling holes, doing build-ups, and plug welding. Additionally, TIG welds are usually softer than stick welds or MIG welds. It can be concluded that TIG welds can be hammered, ground, and formed more easily. If a welder is working with sheet metal and needs to hammer around a welded area, this area is significantly less likely to crack. Since the weld nugget is more malleable, it easier to manage. TIG welding is preferable because it grants increased control over the weld and the possibility to input less heat. Many experiments frequently use TIG welding process parameters such as welding speed, welding current, and filler diameter [11-14].

The plug welding schedule was provided by previous studies [15] and the American Welding Society [16]. According to AASHTO/AWS D1.5M/D1.5: 2002, the plug weld hole diameter must be 8 + t (mm) to achieve weld quality, where t represents thickness of the joined plate (mm). Finding valuable weld schedules for equal-thickness welding is extremely useful. Plug weld quality is significantly affected by important factors such as the area of weld penetration, depth, and strength [17]. Nonetheless, the studies that have focused on plug welding are not abundant [2, 10, 18, 19]. In order to establish plug weld quality, the welds must be loaded in shear while the parts undergo tension loading. In particular cases, the welds can be loaded in tension, with the direction of loading being normal to the joint's plane, or a combination of shear and tension [20].

Strength testing plays an important role within a weldability study and represents an evaluation method as regards automobile body assembly. Among all the tests used to establish weld strength, static tensile-shear testing is by far the most frequent laboratory test. This happens because of its simplicity in specimen testing and fabrication [21]. The tensile-shear testing of a single lap joint workpiece distinguishes from standard homogeneous material testing. According to Zhang and Senkara [3], the results of the tensile test of the weld specimens are not shown in terms of tensile strength (MPa) but as tensile load at break (kN). It was found that specimen width is the most important factor that influences tensile-shear testing. It suffices with an overlap equal to the specimen width [21]. Even though the specimen length plays a less important role, the specimen must be long enough to enable clamping during testing. It was determined that a length of 150 mm is sufficient for all feasible widths [21]. Generally, in the steel and automotive industries, the diameter of a minimum acceptable nugget should range between 4t1/2 and 5t1/2, where t represents the nominal thickness of the sheet in mm [1].

More than often, the experimental optimization of a welding process proves to be a time-consuming and costly task. To solve this problem, the response optimizer method is widely used to determine the group of input variable settings that mutually optimize a set of responses. A full factorial design can trigger optimum process parameters without the need to derive a model for the welding process. Nonetheless, the increase in the number of input parameters leads to an exponential increase in the number of experiments, thus causing the full factorial method to become unrealistic [22]. Recent studies have attempted to address these problems by bringing forth a new approach to experimental optimization [22-24].

The aim of this study is to highlight the importance of the employed welding methods in restoring a damaged vehicle body. Research led into automobile body panel welding focuses chiefly on spot welding and its application in the production process. Plug welding is consistently used to repair damaged automobile body panels. Consequently, this study investigates the degree to which weld quality is influenced by welding parameters on weld quality.

3. METHODOLOGY

3. 1. Experimental Setup Generally, automobile parts use steel sheets of 0.6–2.0 mm thick. The present study focuses on the tensile test of a 1.2 mm thick steel sheet using JIS G3141 SPCC as a base material. JIS G3141 SPCC is a commercial cold-rolled low-carbon steel. SPCC steel is characterized by high weldability and formability. This type of steel is widely used in general applications, frequently in vehicle structures and panels, and significantly in the production of automobile parts (e.g. hoods, roofs, fenders, quarter panels, spring housings, oil pans). See Tables 1 and 2 for the chemical composition of the base material and its mechanical properties.

Test sheets (30 mm wide, 100 mm long) were prepared to comply with the JIS Z3136-1999 standard. Two sheets, with lap joints at the center of the sheets, were stacked and fabricated. As shown in Figure 1, the overall length of the joint part measured 170 mm and the overlap length was 30 mm. in order to determine their failure mode and strength, the welded joints underwent static tensile-shear tests.

3. 2. Spot Weld Procedure Spot welding was done using a TATASU spot welding machine(TOASEIKI SLP-50A5) and a truncated copper electrode with a face diameter of 6.5 mm. The welds were done at room temperature, in open air. Prior to welding, the surfaces of the steel sheets have been cleaned to remove dust, oxides, and grease. This was done to facilitate consistent spot weld quality.

TABLE 1. Chemical composition of JIS G3141 SPCC

C	Mn	P	S
0.04	0.20	0.015	0.006

TABLE 2. Mechanical properties of JIS G3141 SPCC

0.2YS (MPa)	UTS (MPa)	Elongation (%)
164	316	46

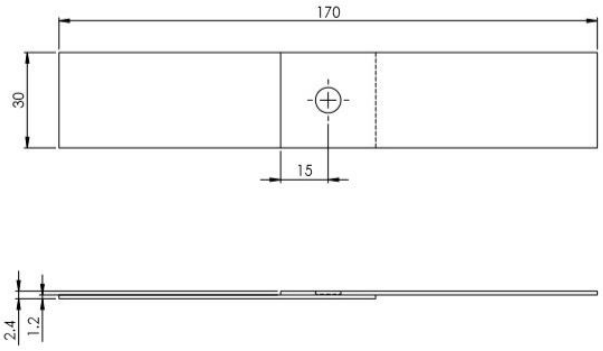

Figure 1. Dimensions of tensile test specimens (mm)

3. 2. 1. Factorial Designs A brainstorming session with personnel from maintenance, quality, design, shop floor, and production was run to identify the process parameters. See Table 3 for the used parameters and their levels.

Therefore, in compliance with the design-of-experiments approach according to which the number of experiments is determined by a full factorial design, various "n = 3" parameters generated eight experiments structured into two levels. To enhance the reliability of the results, we made three replicates that resulted in 24 experiments. The process involved varying the welding time between 8 and 10 cycles, the electrode force between 0.20 and 0.25 Mpa, and the welding current between 70 and 75 kA. For static tensile-shear strength testing, both control factors (i.e. the hold time and the squeeze time) were kept constant at 20 cycles. Figure 2 shows the spot weld specimens of weld-bonded joints before the tensile-shear test.

3. 3. Plug Weld Procedure Prior to welding, the plug-welded joints had to be centered on a 30 mm overlap region. To facilitate TIG plug welding, the outer sheet in all specimens was drilled to obtain round holes. The sheet was afterwards clamped to the back sheet. Binder filling into the hole was used to form the joint. Two low-carbon steel sheets (1.2 mm thick, JIS G3141 SPCC) were plug-welded employing a Panasonic TIG welding machine with argon gas (TIG MINI 150). Due to its extensive industrial application, ER70S-6 filler metal was selected. In compliance with the AWS Specification for Carbon Steel Electrodes and Rods for Gas Shielded Arc Welding (A5.18-2005), ER70S-6 is utilized with thin to medium plate joints. Table 4 lists the standard mechanical properties of the weld metal in the as-welded condition and the standard chemical composition of the solid wire in accordance with AWS requirements.

3. 3. 1. Factorial Designs A brainstorming session with personnel from maintenance, quality, design, shop floor, and production was run to identify the process parameters. The aim of the experiment was to determine the key factors and their possible interactions that affect maximum load. Studying each

TABLE 3. Control factors and their levels used in spot weld

Symbol	Factor (unit)	Level 1	Level 2
A	Welding Current (kA)	70	75
B	Electrode Force (Mpa)	0.2	0.25
C	Welding Time (cycle)	8	10

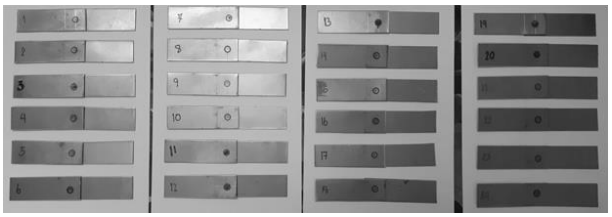

Figure 2. Prepared spot weld specimens before tensile-shear test

parameter involved three levels of control: high, medium, and low. In order to obtain a precise assessment of experimental error (or error variance), each trial condition was repeated three times.

The 3^2 full factorial designs with 3 replications were constituted by twenty-seven weld experiments. The hole diameter varied in a 7-9 mm range and weld current varied in a 100-140 kA range (see Table 5). The diameter of the welding wire and the gas flow rate were kept constant at 1.2 mm and 6 l/s, respectively, during all static tensile-shear strength tests. Figure 3 shows the plug weld specimens of weld-bonded joints prior to tensile-shear test.

3. 4. Tensile-shear Test As Figure 4 shows, in the tensile-shear test, specimens were clamped to a 50 kN Instron universal test machine (Model 5569). The crosshead velocity of 30 mm/min was kept constant, until the final failure of the joint. Maximum load is the most monitored variable in tensile-shear testing [21]. The specimens' failure modes were determined by analyzing the fractured samples.

TABLE 4. Typical chemical and mechanical properties of ER70S-6 in accordance with AWS requirements

C%	0.06-0.15
Si%	0.80-1.15
Mn%	1.40-1.85
P%	0.025 max.
S%	0.035 max.
Cu%	0.50 max.
0.2%OS (MPa)	400 min.
TS (MPa)	480 min.
EI (%)	22 min.
IV (J)	27 min.

TABLE 5. Plug welding control factors and levels

Symbol	Factor (unit)	Level 1	Level 2	Level 3
X	Hole Diameter (mm)	7	8	9
Y	Welding Current (kA)	100	120	140

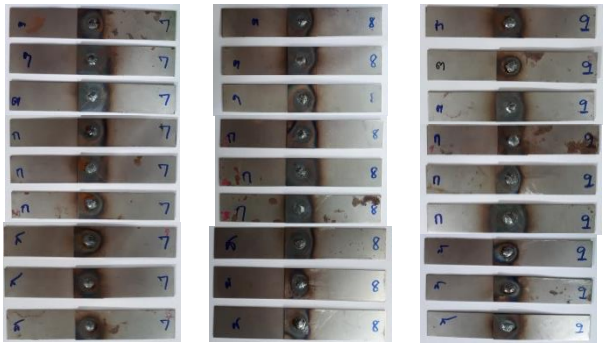

Figure 3. Prepared plug weld specimens before tensile-shear test

Figure 4. Tensile test machine

3. 5. Regression Analysis A regression model corresponding to the subsequent second-order response function was used to perform a multiple regression analysis [25]:

$$y = \beta_0 + \sum_{i=1}^{k} \beta_i x_i + \sum_{i=1}^{k} \beta_{ii} x_i^2 + \sum \sum_{j<i} \beta_j x_i x_j + \varepsilon \quad (1)$$

where β_{ij}, β_{ii}, β_i and β_0 are the coefficients of interaction, quadratic, linear, and intercept variables respectively; y is the response or the dependent variable; x_j and x_i are the independent variables in the coded unit; and ε is the error term that justifies the effects of excluded parameters. The following equation was used for coding [25]:

$$x = \frac{X - (X_{high} + X_{low})/2}{(X_{high} - X_{low})/2} \quad (2)$$

where X is the natural variable, X_{low} and X_{high} are the low and high values of the natural variables, and x is the coded variable. During the analysis, the coefficients that triggered Equation (1) to fit better a set of recollected response variable data acquired from the optimization experiments were established using regression analysis in Minitab. This, effectively generated a regression model that describes the statistical relationship between the response variable and the predictors, and eliminating those predictors

whose statistical relationship with the response variables is not significant. Nonetheless, since the unimportant factor is part of a higher-order term, it was also included.

The model adequacy assessment aims at determining the extent to which all the test data and models agree. The model adequacy was analyzed using a standard probability plot of standardized residuals. Additionally, the global fit of the model was tested through the evaluation of the coefficient of determination (R^2).

3. 6. Optimum Welding Parameters The Minitab optimization feature was employed to establish the optimum welding parameters. Despite the investigations and analyses that were conducted on the response optimizer, estimating the optimized combination of process parameters that allows for the highest possible strength level of the weld strength can be a demanding task. The present study has adopted a GA approach to achieve the optimum combination of process parameters under specific constraints and obtain the highest strength level. GA-based optimization is structured as follows.

Step 1: Create an initial chromosome population arbitrarily.

Step 2: Decode all the chromosomes' genes. For plug welding: (1) welding current, (2) hole diameter. For spot welding: (1) welding time, (2) electrode force, and (3) welding current.

Step 3: Use regression models to determine the weld strength's predicted value.

Step 4: Establish the fitness of all chromosomes; achieve the maximum (fitmax).

Step 5: Conduct the following genetic operations if fit max ≤ required fitness (fit required):

(a) Selection based upon the expected number control method,

(b) Crossover,

(c) Mutation, to create a new chromosome population. Then go to step 2. Otherwise, stop.

Maximizing the weld strength was the objective function. Consequently, the reciprocal of the objective functions was employed as the fitness functions. The potential solutions for an optimization problem are represented by the initial population (individual). Table 6 shows the GA parameters that were used to optimize the parameters of the welding process.

In the present study, the GA is set using the GA toolbox and it is optimized through the MATLAB programming fitness function. GA variables are identified, and the lower and upper bounds of the variables are the following.

As shown below, the spot weld process window for every variable was employed as the boundary constraints.

TABLE 6. Parameters for GA computations

Population size	**50**
Number of generations allowed	1%
Type of mutation	Adaptive feasible
Crossover rate	80%
Type of crossover	Scattered
Type of selection	Roulette wheel

$$70 \leq \text{welding current} \leq 75 \quad (3)$$

$$0.20 \leq \text{electrode force} \leq 0.25 \quad (4)$$

$$8 \leq \text{welding time} \leq 10 \quad (5)$$

As shown below, the plug weld process window for every variable was employed as the boundary constraints.

$$7 \leq \text{hole diameter} \leq 9 \quad (6)$$

$$100 \leq \text{welding current} \leq 140 \quad (7)$$

4. RESULTS AND DISCUSSION

4. 1. Spot Weld Procedure

4. 1. 1. Factorial Design of Welding Parameters Table 7 shows the uncoded design matrix with the corresponding real factor settings and the respective maximum load for the spot weld experiment. In order to create adequate degrees of freedom for the error term, every trial condition was recreated three times. To minimize the effect of undesirable external influences

TABLE 7. Spot weld experimental layout with response values

Run/Trial	**A**	**B**	**C**	**Maximum load (N)**		
				1	**2**	**3**
1	70	0.2	8	6,383	6,511	6,411
2	75	0.2	8	6,958	6,621	6,701
3	70	0.25	8	7,064	7,046	7,107
4	75	0.25	8	7,099	7,213	7,250
5	70	0.2	10	6,894	6,699	6,701
6	75	0.2	10	6,570	6,438	6,536
7	70	0.25	10	7,418	7,379	7,456
8	75	0.25	10	7,355	7,500	7,190

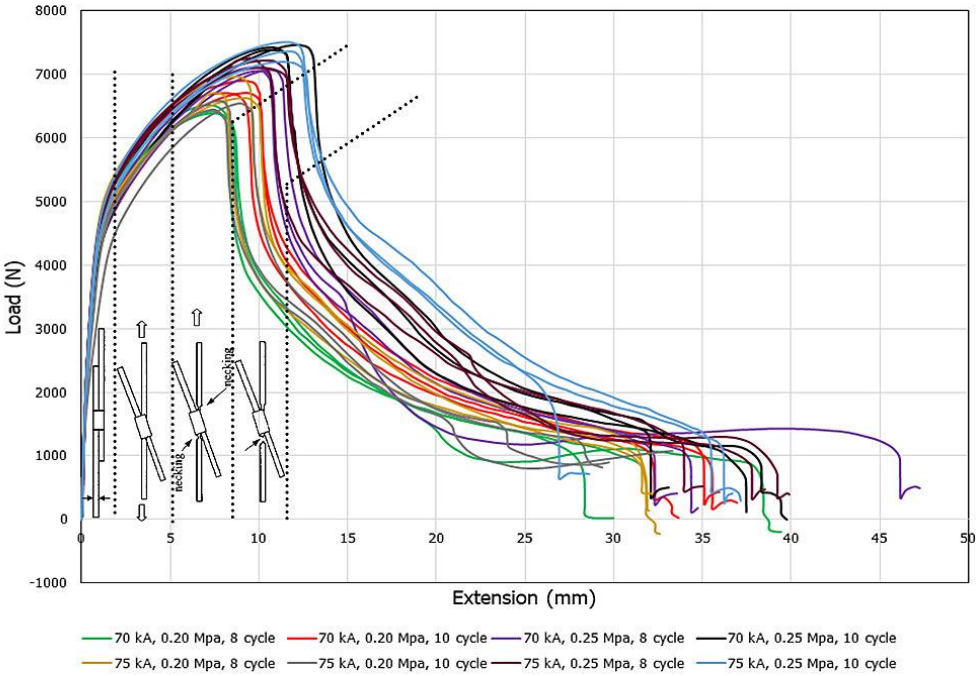

Figure 5. Load vs. extension curves of the spot weld joint

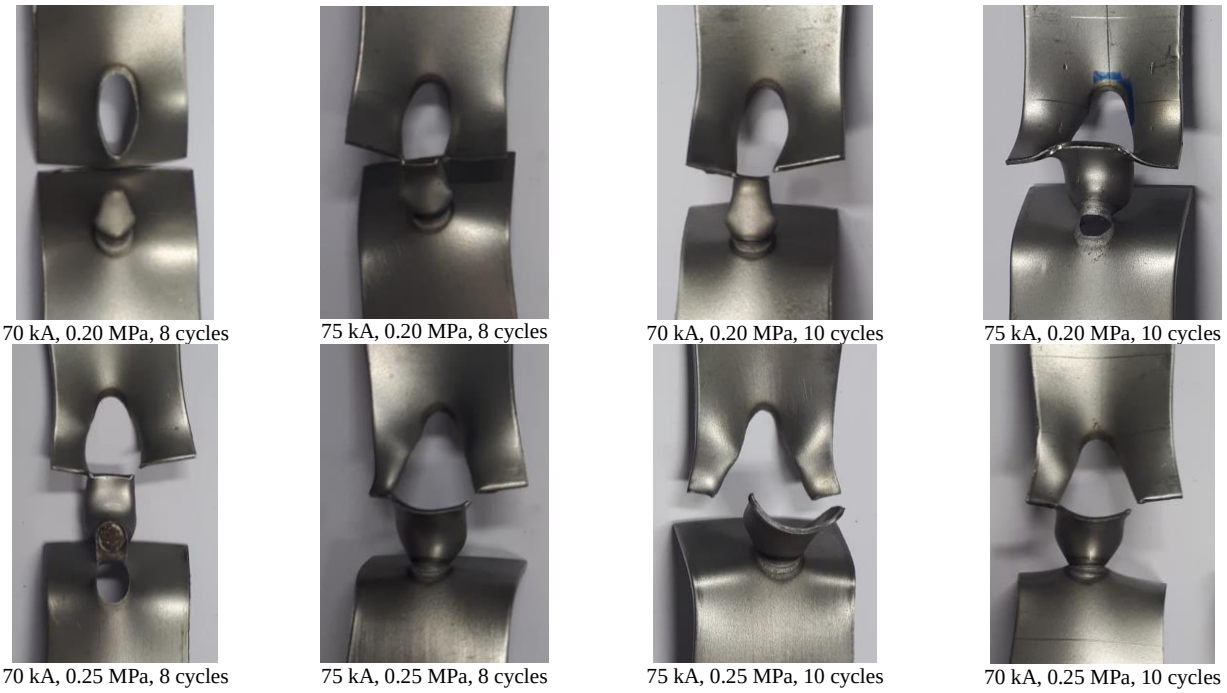

Figure 6. Failure mode of spot-welded samples

and lurking variables induced into the experiment, a randomization strategy was used. The use of the Minitab software allowed to determine which effects influence process variability the most.

Figures 5 and 6, respectively, show the load vs. extension curves and the failure mode of the spot weld joint that were generated in the experiments. In the lap-shear test, as shown in Figure 5, the load vs. extension curve illustrates a nonlinear region before the maximum load is reached. Initially, the welded joint is pulled parallel to the force direction. The nugget rotates in order to align with the applied force direction. As the

load increases, localized necking of the sheet metal occurs at locations near the boundary of the base metal and the nugget. Once the maximum load is reached, the load begins to drop when the crack initiates and gradually decreases as the base metal tears around the weld nugget. Figure 6 displays the gradual changing trend in the growing order of the maximum loads. Higher forces and shorter times should be used conjointly. Higher welding current is necessary at shorter welding times. The necessary current depends on the size of the used electrode tip, the other parameters set, and the material type. If the current is low, the strength of the weld joint will be insufficient due to the brittleness of the created nugget. Since the welding current was continuously increased, the nugget diameter reached a maximum increase initially and then decreased progressively due to excessive splashing and melting. An adequate welding time setting would provide a good welding contact without generating burn marks on the workpiece surface and significant deformation. The transformation was complemented by a hardness decrease in the heat-affected zones of the welds and the nugget. As far as the welding force setup is concerned, improper welding force can cause a weak connection between the welding surfaces, thus generating metal splash and poor weld results. The higher the welding force of the electrode is, the greater the deformation on the workpieces will be. Due to this transformation, the current flows along different paths instead of a small spot generating a wide array of temperature distributions in the workpieces.

Regarding the failure modes, as presented in the ISO standards [26], in weld quality testing, all specimens coincide with the tearing of the base metal because the quantitative measurement of weld strength is attainable. Additionally, failure modes show if the size of the specimen is appropriate [21].

4. 1. 2. Regression Model Regression analysis sees the effect of a factor defined as the change in response caused by a change in the factor's level. Since it refers to the main factors of interest in the experiment, it is commonly called a main effect. Equation (8) gives the mathematical model for factorial design 2^3, where N represents the mean of the maximum load, while A, B, and C indicate welding current, electrode force, welding time, respectively. Since the experimental results model ensures a good correlation (R^2 = 92.61%), all the coefficients for the subsequent mathematical model were evaluated in the coded format. If the statistical model (R^2 (adj) = 90.55%) is adjusted, these values denote the percentage of data detected in the response and that can be explained by the mathematical model.

$$N = -17536 + 347.8A - 6247B + 2352C \\ -37.97A*C + 2111B*C \quad (8)$$

4. 1. 3. Model Adequacy Checking Figure 7 shows the ANOVA for the complete 2^3 factorial designs with three replicates. The obtained data shows that the main effects of welding time and electrode force are relevant for the maximum load. However, the welding current is not relevant, as it displays values over the significance level of (5%). The relationship between electrode force*welding time and welding current*welding time are relevant as the p-value is inferior to the significance level used at the 5% probability level ($p < 0.05$).

The analysis of a 2^k factorial design presumes that the observations are assigned normally and independently. Producing a normal probability plot of residuals is the most appropriate way to verify the normality assumption. As shown in Figure 8, the residual plot for the maximum load response is characterized as a significant procedure to guarantee that the developed mathematical models continually illustrate the responses of interest.

Factorial Regression: Max Load (N) versus Welding Current , Electrode Force , Welding Time

Backward Elimination of Terms

α to remove = 0.05

Analysis of Variance

Source	DF	Adj SS	Adj MS	F-Value	P-Value
Model	5	2860293	572059	45.09	0.000
Linear	3	2577162	859054	67.71	0.000
Welding Current (kA)	1	5494	5494	0.43	0.519
Electrode Force (Mpa)	1	2440816	2440816	192.39	0.000
Welding Time	1	130852	130852	10.31	0.005
2-Way Interactions	2	283131	141566	11.16	0.001
Welding Current (kA)*Welding Time	1	216260	216260	17.05	0.001
Electrode Force (Mpa)*Welding Time	1	66871	66871	5.27	0.034
Error	18	228359	12687		
Lack-of-Fit	2	57370	28685	2.68	0.099
Pure Error	16	170989	10687		
Total	23	3088651			

Model Summary

S	R-sq	R-sq(adj)	R-sq(pred)
112.635	92.61%	90.55%	86.86%

Figure 7. ANOVA results for the full factorial experiments with Table 7

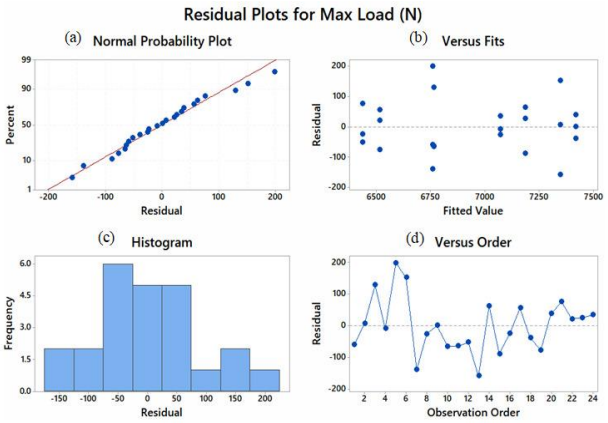

Figure 8. Residual plot for the spot weld experiment, (a) normal probability plots of residuals, (b) residuals versus fits plots, (c) histogram of residuals, and (d) residuals versus observation order

Typically, ANOVA assumptions are checked using four main diagnostic plots: (a) residuals versus the order, (b) histogram of standardized residuals, (c) versus fits for standardized residuals, and (d) normal probability plot for standardized residuals. Should these assumptions be satisfied, then standard least-squares regression will generate objective coefficient estimates with minimum variance. Figure 8a shows that residuals relatively fall along a straight line. Consequently, the normal distribution assumption is considered as satisfied. As shown in Figure 8b, all residual points are dispersed within lower and upper bounds, showing no pattern. This plot denotes that the independence assumption is also satisfied. The histogram shown in Figure 8c apparently forms a normal curve equally distributed around zero, showing that the normality assumption is more than likely true. Since Figure 8d shows that all residual points are spread irregularly over the graph within the lower and upper bounds showing no evident patterns, the assumption according to which residuals have a regular variance is confirmed. As a result, all diagnostic plots denote that all the necessary ANOVA assumptions are satisfied.

As shown in Figure 9, a Pareto plot can illustrate statistically significant effects. The interactions or factors on the outside of the dotted line at 2.12 are relevant in decreasing order: electrode force, welding time, welding current*welding time interaction electrode force*welding time interaction, and lastly, welding current*electrode force*welding time interaction. Put differently, these effects have significant impact on the mean maximum load, even if the welding current has no relevant impact on the mean maximum load. This result can be further supported by taking into consideration the main effects plot and interaction plot (as shown in Figures 10 and 11, respectively).

Figure 10 shows a graphic representation of the primary effects of the spot weld examined factors in regard to maximum load. According to the graph, it can be concluded that a factor is directly linked to the slope and length of the line in the graphic. The greater the slope is, the higher the influence on the average maximum load increase will be when varying levels from low to high. Therefore, when these primary effects result from a 90.55% statistical adjustment, with a p-value inferior to 5% significance (representing a 95% confidence level), these results are valid for this spot procedure.

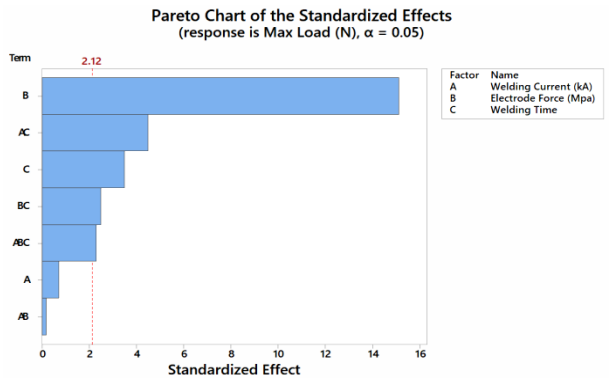

Figure 9. Pareto plot of effects on maximum load variability

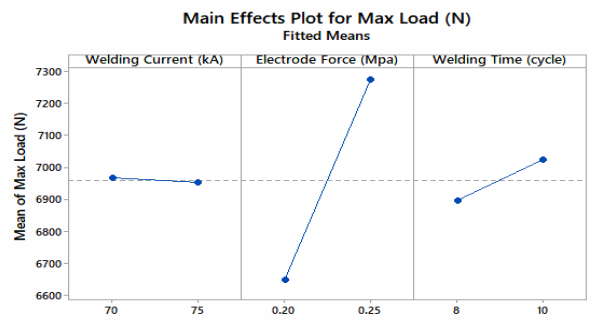

Figure 10. Main effects plot for spot weld experiment

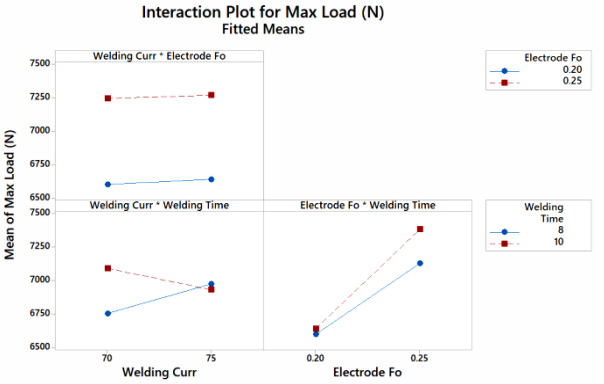

Figure 11. Interaction plot for the spot weld experiment

According to Figure 10, the electrode force has a significant impact on maximum load, while welding current has absolutely no impact due to the lower slope. Nonetheless, it should be noted that welding time is less sensitive to variability in maximum load if compared to electrode force.

As shown in Figure 11, the three two-factor interaction graphics denote a powerful interaction between "electrode force*welding time." Maximum load reaches its highest when welding time and electrode force are kept at a high level, i.e. 10 cycles and 0.25 MPa, respectively. Likewise, maximum load reaches its minimum when welding time and electrode force both maintain a low level, i.e. 8 cycles and 0.20 MPa, respectively.

4. 1. 4. Determination of Optimum Parameters Regression Model To establish the optimal conditions of maximum load, an optimization study is necessary. As soon as the model has been developed

and verified for adequacy, the optimization criteria must be set to determine the optimum conditions. In order to establish the combination of input variable settings that conjointly optimize a response, a response optimizer was employed. Consequently, 7,463 N was the predicted maximum load value.

As Figure 12 shows, the optimum parameters detected in uncoded units were weld time of 10 cycles, electrode force of 0.25 MPa, and weld current at 70 kA. As a final step, the confirmation test experiment must be conducted. To assess the accurateness of the value predicted by the suggested GA (see Figure 13), an experiment was conducted based upon the optimized process parameters.

The experiments carried out under the optimum conditions were replicated three times. The average value for maximum load turned out to be 7,348 N. The results in Table 8 clearly show that the GA predicted

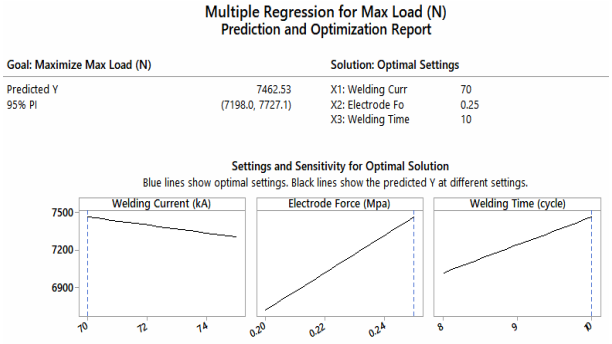

Figure 12. Response optimizer for the spot weld experiment

TABLE 8. Predicted maximum load of spot weld under optimum process parameters and experiment value

Predicted value by Response optimizer	**7.463**
Predicted value by GA	7.467
Experiment value	7.348

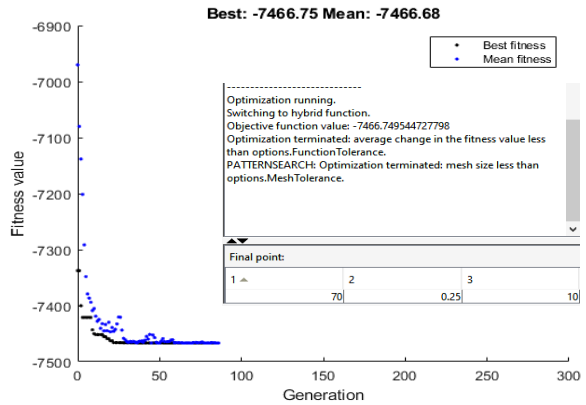

Figure 13. GA convergence plot for the optimal load of the spot weld

value is suitably close to the practical value that was obtained experimentally.

4. 2. Plug Weld Procedure

4. 2. 1. Factorial Design of Welding Parameters

An experimental layout that included all combinations of plug weld parameters and their respective levels was constructed to identify the significant interaction and main effects. Table 9 displays the real settings of the process parameters and the response values that were registered at each trial condition. As showed in Run/Trail 6, achieving weld accuracy and deeper penetration in plug welding of thin sheet metal demands experienced welders. The degree of experience and skill of the welder may affect the weld quality.

The failure mode of welded samples and load vs. extension curves derived from the plug weld joint tests can be found in Table 10 and Figure 14, respectively. The original crack formed after maximum load, whereas the rear sheet started to fold. In the configuration after the full separation, a button spawned from the thin sheet. The thin sheet behind the button was pulled away from the remaining thin sheet. As the welding current and hole diameter increased, tensile-shear load also increased. The shape of the curve's "tail" relies on the post-failure mode. A long tail correlates with an interfacial failure, usually one-half button pullout and consequential tearing of the base metal alongside the loading direction. A short tail corresponds to a full button pullout [27]. Immediately after failure, the load drops to zero. The failure mode is usually a complete and clean button pullout.

The failure of the plug-welded sample, as shown in Figure 14, Failure Modes A, B and C correspond to pull-out failure, tearing of the base metal and interfacial failure. In Failure Mode A, the nugget rotates and the tensile load is increased, and then the localized necking occurs outside the nugget, resulting in crack

TABLE 9. Plug weld experimental layout with response values

Run/Trial	**X**	**Y**	**Maximum load (N)**		
			1	**2**	**3**
1	7	100	3.019	3.327	3.066
2	8	100	5.501	5.773	5.587
3	9	100	5.745	5.694	6.918
4	7	120	4.834	4.497	4.970
5	8	120	5.711	6.484	5.876
6	9	120	7.817	9.201	7.671
7	7	140	5.220	5.946	5.862
8	8	140	5.757	5.483	6.468
9	9	140	8.607	8.737	7.887

TABLE 10. Failure mode of plug-welded samples

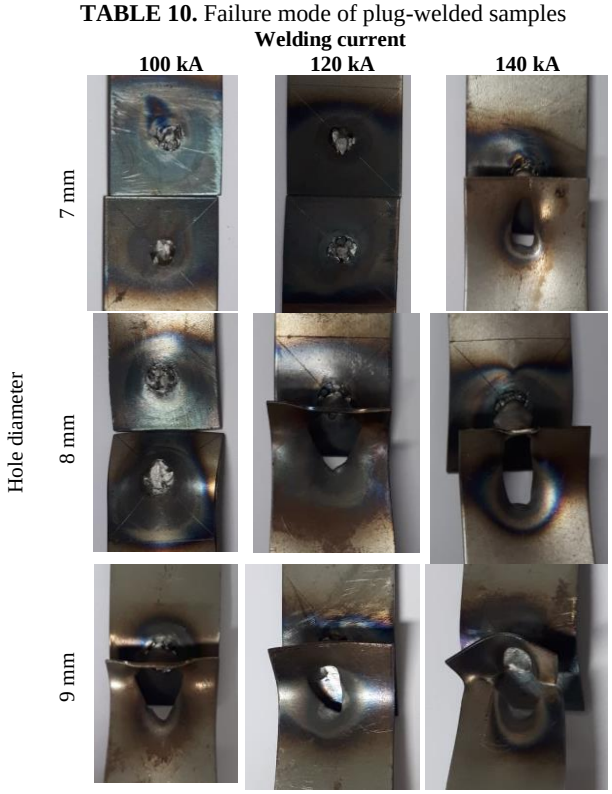

initiations around the nugget's periphery, while in Failure Mode C, failure occurs by crack propagation through the nugget. In the case of Failure Mode B, failure occurs by weld nugget being partially pulled out from the base metal. Plug-welded material with a 7 mm hole diameter had low tensile-shear strength because of the low penetration size, leading to interfacial failure. The increment in tensile-shear load with increasing hole diameter was mainly attributed to the growth of penetration size. Assumedly, tensile-shear load increased when the hole diameter was incresed to 8 mm.

4. 2. 2. Regression Model Equation (9) gives the mathematical model for factorial design 3^2 terms of un-coded factors, where N represents the mean of the maximum load, and Y and X are the welding current and mean hole diameter, respectively. For the subsequent mathematical model, all coefficients have been estimated in their coded format, as derived from the experimental results. Additionally, the model ensures a good correlation (R^2 = 93.71%). Adjusting the statistical model (R^2 (adj) = 90.92%) allows for these values to explain the variability to 90.92%.

$$N = -30058 + 1530X + 360Y - 1.323Y^2 \quad (9)$$

4. 2. 3. Model Adequacy Checking Figure 15 provides the ANOVA results for the complete 3^2 factorial designs with three replicates. The data shows that the main effects of welding current and hole diameter are relevant for the maximum load. Since the p-value is inferior to the significance level established at 5% probability level ($p < 0.05$), the interaction between hole diameter*welding current can be considered significant. For compelling statistical conclusions, the ANOVA assumptions should be verified and tested using model diagnostic plots. A normal probability plot was used to test the normality of the data.

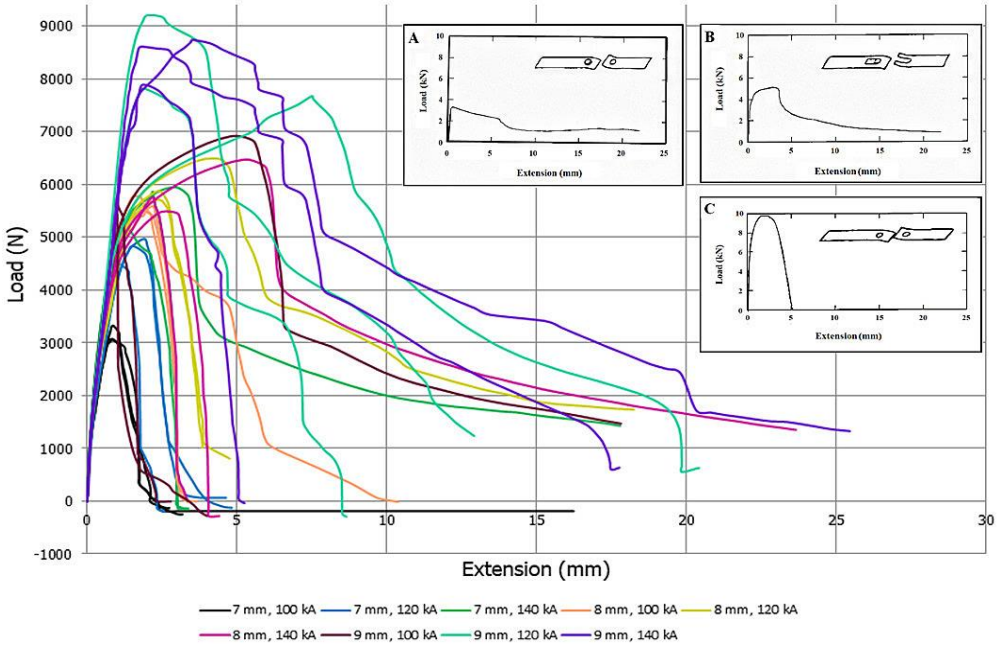

Figure 14. Load vs. extension curves of the plug weld joint

In Figure 16a, a normal probability plot is shown, revealing that the residuals fall on a straight line, indicating normal distribution. Figure 16b shows predicted plot versus residuals. Figure 16b displays the fitted response values versus the variation of the residuals. It is obvious that the data points distribution is random (patternless), indicating that error independency and variance constancy are valid. The plot of residuals versus order was used to verify lurking variables that could have influenced the response throughout the experiment. Apparently, the histogram shown in Figure 16c forms a normal curve equally distributed around zero, indicating that the normality assumption is more than likely true. Additionally, a variation of the residuals versus the run order was plotted to test data independence (Figure 16d). As expected for normally distributed data, it clearly indicated a random scatter. Considering the above discussion, it is obvious that the ANOVA assumptions, namely variance constancy, error independency, and error normality are validated. The normal plot for standardized effects can only be applied to 2^k designs and not to general factorial designs. Generally, factorial designs should be used to choose interaction terms and vital main effects rather than standardized effects (also called normalized effects). Figure 17 shows one of the effects of welding parameters on tensile-shear test samples. As shown, modifying the hole diameter from 7 mm to 9 mm caused a greater main effect than welding current.

Figure 18 reveals a strong interaction between welding current and hole diameter. It is obvious that the effect of the hole diameter at varying levels of welding current is different. Yield is maximum if welding current and hole diameter are maintained high levels, i.e., 140 kA and 9 mm, respectively.

General Factorial Regression: Max Load (N) versus Diameter (mm), Welding Current (kA)

Factor Information

Factor	Levels	Values
Diameter (mm)	3	7, 8, 9
Welding Current (kA)	3	100, 120, 140

Backward Elimination of Terms

α to remove = 0.05

Analysis of Variance

Source	DF	Adj SS	Adj MS	F-Value	P-Value
Model	8	62308829	7788604	33.54	0.000
Linear	4	57136493	14284123	61.52	0.000
Diameter (mm)	2	42388974	21194487	91.28	0.000
Welding Current (kA)	2	14747519	7373760	31.76	0.000
2-Way Interactions	4	5172336	1293084	5.57	0.004
Diameter (mm)*Welding Current (kA)	4	5172336	1293084	5.57	0.004
Error	18	4179648	232203		
Total	26	66488477			

Model Summary

S	R-sq	R-sq(adj)	R-sq(pred)
481.874	93.71%	90.92%	85.86%

Figure 15. ANOVA results for the full factorial experiments with Table 9

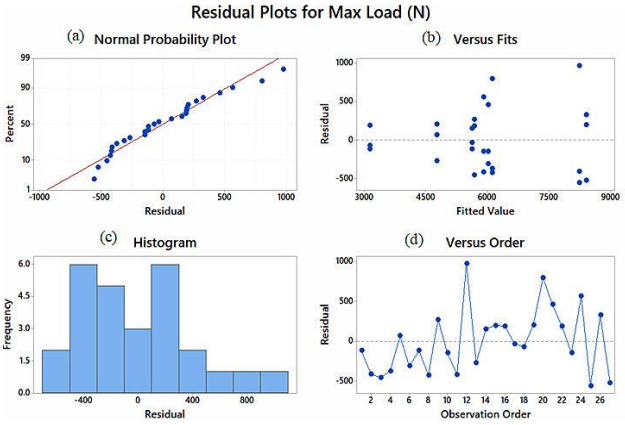

Figure 16. Residual plot for the plug weld experiment, (a) normal probability plots of residuals, (b) residuals versus fits plots, (c) histogram of residuals, and (d) residuals versus observation order

4. 2. 4. Determination of Optimum Parameters

Figure 19 displays the optimal process conditions necessary to produce maximum load under specific conditions. The optimum conditions for maximum load yield as estimated by the response optimizer were welding current 140 kA and hole diameter 9 mm. at optimal conditions, the maximum value for tensile-shear strength was calculated at 8,213 N.

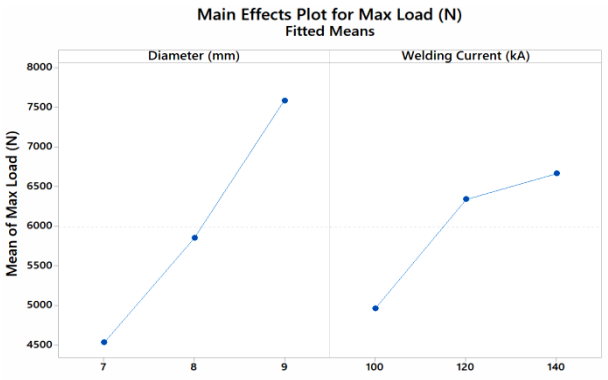

Figure 17. Main effects plot for the plug weld experiment

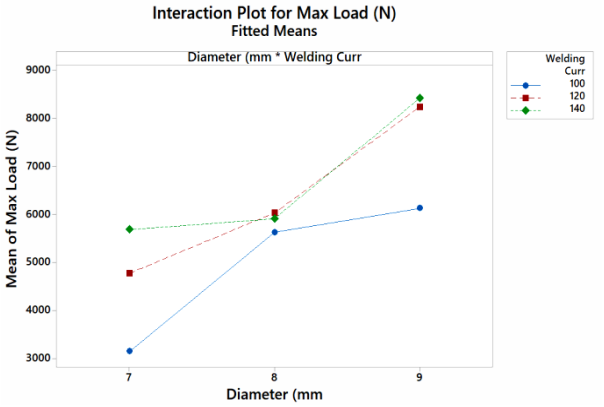

Figure 18. Interaction plot for the plug weld experiment

As Figure 20 shows, if the optimization problem is solved, the GA supplies optimum combinations of parameters to achieve maximum weld strength compared to the original set of welding parameters.

In order to confirm the accuracy of the established response optimizer function, three replicates of batch experiments have been conducted at optimal conditions. With nonlinear functions, optimum values may take place at the boundaries or in-between them. In the experiment conducted under optimal conditions, 8,262 N was the average value for maximum load.

Table 11 shows optimum welding conditions that lead to the maximum weld strength. The optimization results have been verified against factual experimental data, revealing that they are satisfactory.

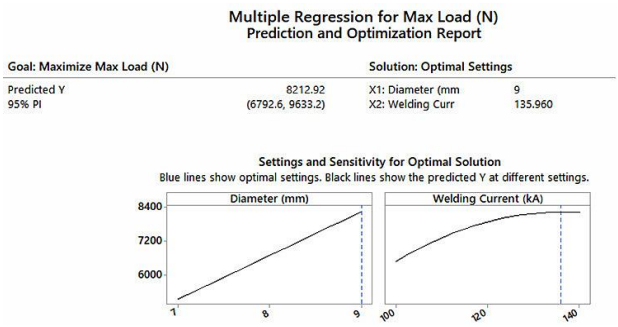

Figure 19. Response optimizer for the plug weld experiment

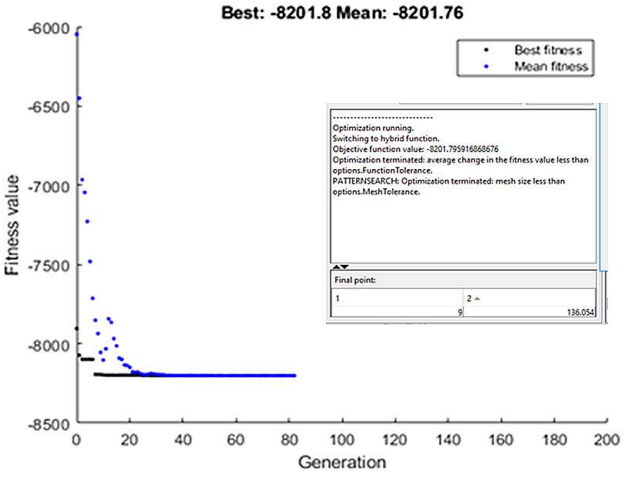

Figure 20. GA convergence plot for the optimal load of plug weld

TABLE 11. Predicted maximum load of plug weld under optimum process parameters and experiment value

	Hole diameter (mm)	Welding current (kA)	Maximum load (N)
RSM	9	135.960	8,213
GA	9	136.054	8,202
Experiment	9	136	8,262

5. CONCLUSIONS

The aim of this study was to evaluate the characteristics of plug welding and spot welding used in the vehicle body panel restoration process. The shear tension of welds was analyzed experimentally. Based on the statistical analysis and experimental results, the conclusions derived from the current investigation are summarized thusly.

The optimal spot welding parameters necessary to produce a maximum load of 7.4 kN were an electrode force of 0.25 MPa, a welding current of 70 kA, and a welding time of 10 cycles. The failure modes detected during tensile-shear testing caused full button failure tearing of the base metal in all tests. The JIS G3141 SPCC resistance factor is higher. Consequently, the current requirements are slightly lower. Because of the additional compressive strength that is inherent in JIS G3141 SPCC, electrode force is usually higher with this type of materials. Since metallurgical changes are greater with this type of materials, welding time is more critical. When welding this type of materials, it is advisable to employ longer welding times to permit more ductile welds and reduce the cooling rate.

The optimal plug welding parameters necessary to produce an 8.2 kN maximum load were a welding current of 136 kA and a hole diameter of 9 mm. The failure of the plug-welded sample happens in three modes: interfacial failure, tearing of the base metal, and button pullout. Plug welds are exceptionally tough and will not fail unexpectedly. Small diameter plug welds may be difficult. Full fusion achievement requires adequately trained and skilled welders. According to the recommendations provided by AWS, the minimum hole diameter necessary to guarantee the reliability of plug-welded materials based on 1 mm thin joined materials is 9 mm. Based on the 2 mm average joined material thickness, the minimum hole diameter must be 10 mm. The results show that the formula for plug weld proposed by AWS can be used for similar plug-welded metals with equal-thickness welding. Strengths were proportional to the amount of current. In order to ensure complete fusion and achieve the shear strength of the weld metal, the highest practical welding current for the used electrodes should be used for plug welds. This strength increase with welding current confirms the theory according to which ultimate shear strength relies on the amount of penetration.

In the case of spot welding, the test numbers that exceeded an upper limit caused burnt workpieces. In the case of values below the lower limit, the finished workpieces were non-adjacent. This experiment used thin sheets as plug welding specimens. A hole diameter above 9 mm would burn the joints. However, penetration does not occur if the hole diameter is less than 7 mm. Additionally, a welding current above 140

kA may burn the workpiece. Consequently, the optimum welding parameters in the present study are fit for joining similar SPCC steel sheet (1.2 mm thick) to attain the higher load value that complies with the actual engineering conditions.

The aim of this pilot study was to estimate the main parameters for the welding process of automotive body panels. The results can help manufacturers understand which parameters require less attention, narrower ranges, or tighter control. Lastly, this study will distinctly separate non-key from key parameters. If a process parameter that has been tested over this range presents no relevant effect on process performance, it is safe to consider it a non-key parameter. Nonetheless, even if digressions from these process parameters present no weldability impact, it is advisable to monitor them to guarantee consistent process control. Parameters with a measurable, significant effect are considered key parameters that must be tested in future sets of characterization experiments. The results of this study are expected to be applied to upcoming studies on practical optimization for repair and maintenance of automotive body panels.

6. ACKNOWLEDGMENT

This present research is funded by Faculty of Technical Education, King Mongkut's University of Technology North Bangkok, (contract No. FTE-2563-04).

7. REFERENCES

1. Mallick, P., Joining for lightweight vehicles, in Materials, design and manufacturing for lightweight vehicles. 2010, Elsevier.275-308. doi: 10.1533/9781845697822.2.275
2. Kwon, J., Kim, J. and Lee, Y., "Experimental study on spot weld and plug weld of automotive body panel", ***Transactions of the Korean Society of Automotive Engineers***, Vol. 24, No. 6, (2016), 709-715. doi: 10.7467/KSAE.2016.24.6.709
3. Zhang, H. and Senkara, J., "Resistance welding: Fundamentals and applications, CRC press, (2011).
4. Duffy, J.E., "Auto body repair technology, Cengage Learning, (2014).
5. Jou, M., "Real time monitoring weld quality of resistance spot welding for the fabrication of sheet metal assemblies", ***Journal of Materials Processing Technology***, Vol. 132, No. 1-3, (2003), 102-113. doi: 10.1016/S0924-0136(02)00409-0
6. Farrahi, G.H., Kashyzadeh, K.R., Minaei, M., Sharifpour, A. and Riazi, S., "Analysis of resistance spot welding process parameters effect on the weld quality of three-steel sheets used in automotive industry: Experimental and finite element simulation", ***International Journal of Engineering, Transactions A: Basics,*** Vol. 33, No. 1, (2020), 148-157. doi: 10.5829/ije.2020.33.01a.17
7. Özyürek, D., "An effect of weld current and weld atmosphere on the resistance spot weldability of 304l austenitic stainless steel", ***Materials & Design***, Vol. 29, No. 3, (2008), 597-603. doi: 10.1016/j.matdes.2007.03.008
8. Darwish, S. and Al-Dekhial, S., "Micro-hardness of spot welded (bs 1050) commercial aluminium as correlated with welding variables and strength attributes", ***Journal of Materials Processing Technology***, Vol. 91, No. 1-3, (1999), 43-51. doi: 10.1016/S0924-0136(98)00414-2
9. Jamaludin, S.B., Hisyam, M., Shamsudin, S.R., Darus, M. and Wahid, M.F.M., "Study of spot welding of austenitic stainless steel type 304", ***Journal of Applied Sciences Research***, Vol. 3, No. 11, (2007), 1494-1499.
10. Gibson, G.J., "An investigation of plug and slot welds", M. S. Thesis, Lehigh University, (1937).
11. Gopinath, V., Manojkumar, T., Sirajudeen, I., Yogeshwaran, S. and Chandran, V., "Optimization of process parameters in tig welding of aisi 202 stainless steel using response surface methodology", ***International Journal of Applied Science and Engineering Research***, Vol. 10, No. 13, (2015), 11053-11057.
12. Srirangan, A.K. and Paulraj, S., "Multi-response optimization of process parameters for tig welding of incoloy 800ht by taguchi grey relational analysis", ***Engineering Science and Technology, an International Journal***, Vol. 19, No. 2, (2016), 811-817. doi: 10.1016/j.jestch.2015.10.003
13. Simhachalam, D., Rao, M. and Raju, B.N., "Evaluation of mechanical properties of stainless steel (ss 304) by tig welding at heat affected zone", ***International Journal of Engineering and Management Research***, Vol. 5, No. 4, (2015), 214-221.
14. Duhan, R., "Effect of activated flux on properties of ss 304 using tig welding", ***International Journal of Engineering, Transactions B: Applications,*** Vol. 28, No. 2, (2015), 290-295. doi: 10.5829/idosi.ije.2015.28.02b.16
15. Tsuruta, A., Arai, Y. and Tanaka, R., "On the strength of plug welding of thin steel sheets", ***Journal of The Japan Welding Society***, Vol. 21, No. 5-7, (1952), 144-149. doi: 10.2207/qjjws1943.21.144: doi: 10.2207/qjjws1943.21.144.
16. Committee, A.W.S.S.W., Society, A.W. and Institute, A.N.S., "Structural welding code--steel, Amer Welding Society, (1994).
17. O'Brien, A. and Guzman, C., "Welding handbook: Welding processes, American Welding Society, (2007).
18. Ilman, M.N. and Soekrisno, R., "Static and fatigue behavior of plug-welded dissimilar metal welds between carbon steel and austenitic stainless steel with different thicknesses", ***International Journal of Mechanical and Materials Engineering***, Vol. 9, No. 1, (2014), 17. doi: 10.1186/s40712-014-0017-4
19. Hadryś, D., "Mechanical properties of plug welds after micro-jet cooling", ***Archives of Metallurgy and Materials***, Vol. 61, No. 4, (2016), 1771-1776. doi: 10.1515/amm-2016-0286
20. Hasanbaşoğlu, A. and Kaçar, R., "Resistance spot weldability of dissimilar materials (aisi 316l–din en 10130-99 steels)", ***Materials & design***, Vol. 28, No. 6, (2007), 1794-1800. doi: 10.1016/j.matdes.2006.05.013
21. Zhou, M., Hu, S. and Zhang, H., "Critical specimen sizes for tensile-shear testing of steel sheets", ***Welding Journal-New York-***, Vol. 78, (1999), 305-s.
22. Kim, D. and Rhee, S., "Optimization of arc welding process parameters using a genetic algorithm", ***Welding Journal (Miami, Fla)***, Vol. 80, No. 7, (2001), 184s-189s.
23. Correia, D., Gonçalves, C., Junior, S.S. and Ferraresi, V., "Gmaw welding optimization using genetic algorithms", ***Journal of the Brazilian society of Mechanical Sciences and Engineering***, Vol. 26, No. 1, (2004), 28-32. doi: 10.1590/S1678-58782004000100005
24. Perez Pozo, L., Olivares Z, F. and Durán A, O., "Optimization of welding parameters using a genetic algorithm: A robotic arm–assisted implementation for recovery of pelton turbine blades", ***Advances in Mechanical Engineering***, Vol. 7, No. 11, (2015), 1687814015617669. doi: 10.1177/1687814015617669

25. Myers, R.H., Montgomery, D.C. and Anderson-Cook, C.M., "Response surface methodology: Process and product optimization using designed experiments, John Wiley & Sons, (2016).
26. Association, J.S., "Specimens dimensions and procedure for shear testing resistance spot and embossed projection welded joints", Japanese Standards Association. Japan, JIS, 3136, (1999).
27. Chao, Y.J., "Ultimate strength and failure mechanism of resistance spot weld subjected to tensile, shear, or combined tensile/shear loads", ***Journal of Engineering Materials and Technology***, Vol. 125, No. 2, (2003), 125-132. doi: 10.1115/1.1555648.

Persian Abstract

چکیده

جوش‌کاری نقطه‌ای مقاومتی یک فرایند اساسی جوش‌کاری است که در مونتاژ بدنه‌ی خودرو استفاده می‌شود. البته، جوش‌کاری دکمه‌ای به دلیل سادگی فنی و مزایای آن در تعمیر بدنه‌ی خودرو کاربردهای زیادی دارد. در این مقاله، جوش‌کاری نقطه‌ای و دکمه‌ای با استفاده از جوش‌کاری تنگستن–گاز بی‌اثر (TIG) برای پانل بدنه‌ی خودرو مقایسه شده است. جوش‌کاری TIG برای جوش‌کاری دکمه‌ای انتخاب می‌شود زیرا بیشترین انعطاف‌پذیری را برای جوش‌کاری گسترده‌ترین طیف مواد، ضخامت و انواع آن فراهم می‌کند. ماده‌ی پایه‌ی مورد استفاده در این مطالعه JIS G3141 SPCC است. برای تعیین اهمیت پارامترهای فرایند، از طرح آزمایشی فاکتوریل کامل همراه با تحلیل آماری و گرافیکی نتایج با استفاده از تحلیل واریانس استفاده شد. اندرکنش پارامترها با استفاده از تحلیل رگرسیون، بررسی کفایت مدل و تعیین شرایط بهینه بررسی شد. از الگوریتم ژنتیک برای پیش‌بینی ترکیب بهینه‌ی پارامترهای فرایند برای تحقق بالاترین سطح مقاومت استفاده می‌شود. برای مقاومت در برابر کشش، نتایج آزمایش نشان می‌دهد که بیشینه‌ی بار جوش‌کاری دکمه‌ای بالاتر از جوش‌کاری نقطه‌ای است. اتصالات بهینه‌ی جوش‌کاری دکمه‌ای در قطر سوراخ ۹ میلی‌متر و جریان ۱۳٦ کیلو آمپر، با حداکثر بار ۸.۲ کیلو نیوتن به دست آمد. بیشترین بار اتصال جوش نقطه‌ای۷.٤ کیلو نیوتن، در جریان ۷۰ کیلو آمپر، نیروی الکترود ۰.۲۵ مگاپاسکال و ۱۰ چرخه زمان جوش‌کاری مشاهده شد.